ELSEVIER

Journal of Nuclear Materials 241–243 (1997) 328–332

journal of nuclear materials

Temperature profiles in stochastic boundaries

Samuel Féron *, Philippe Ghendrih

Association Euratom-CEA, DRFC, CE Cadarache, 13108 St. Paul-lez-Durance cedex, France

Abstract

During ergodic divertor operation, strong poloidal and radial modulations of the temperature field have been observed in stochastic boundaries. Using field line tracing, one finds that steady state modulations are governed by field lines stochasticity. A 1D radial model is proposed, based on a superimposition of two coupled diffusive networks, a first one standing for the transverse diffusion and a second one accounting for the effects of the stochastic parallel transport. Modulations are then recovered under some conditions. The model predicts that the temperature in the core plasma is not affected by the divertor, which is experimentally verified.

Keywords: Ergodic divertor; Stochastic boundary; Analytic 1D model; Energy balance; Transverse transport

1. Introduction

On Tore Supra, heat extraction and edge plasma control can be organized by a specific configuration, the ergodic divertor. A set of coils induces an external radial magnetic perturbation which presents a toroidal and poloidal spectrum depending on the magnetic equilibrium and on the external current level. The spectrum is characterized by a main toroidal wave number $n = 6$ and by poloidal wave numbers from $m = 12$ to $m = 24$. This configuration governs resonant radial modes which are only significant in a specific volume defining the perturbed region. For a sufficiently high level of the perturbation, magnetic surfaces are destroyed in this volume, so that the heat diffusion process is considerably increased.

In this paper, we analyze the transport of energy in the stochastic volume. We pay a special attention to the fact that this volume is finite and therefore sensitive to the boundary conditions. The latter are an influx of energy at the core boundary and a sink at the wall, volume losses such as radiation are not considered. Although we emphasize ergodic divertor issues, similar features are to be found in others configurations (axisymmetric divertor and stellarators).

In Section 2, experimental results are presented, showing a temperature behaviour characterized by poloidal and radial modulations and a temperature in the plasma core which is not affected by divertor effects. In Section 3, the main properties of the magnetic perturbation are investigated using the field line tracing code Mastoc [4]. A 1D model is then introduced (Section 4) and allows one to compare the limiter and divertor configurations. We find that the modulations are recovered and explained by the model. The transition between the stochastic and unperturbed volume is also analyzed and a local confining pinch velocity is found.

2. Limiter and divertor temperature profile

In the following, the temperature field is modelled by test particles. The test particles density stands therefore for the energy and hence for the plasma temperature at constant electron and ion density.

Let us consider a simple 1D diffusion model with no volume sources and sinks. The sources and sinks at the boundaries are characterized by an energy influx at $r = r_0$ and an energy outflux at $r = L$. One then expects a monotonous and decreasing temperature profile given by, assuming a constant diffusion coefficient $D_\perp$:

$$T(r) = \frac{\Gamma}{D_\perp}(L - r) = T_{\lim}(r) \tag{1}$$

where Γ the influx and L the diffusion area width. This

* Corresponding author. Tel.: +33-4 42 25 40 25; e-mail: feron@drfc.cad.cea.fr.

PII S0022-3115(96)00523-5

situation is typical of limiter and axisymmetric divertor configurations.

In contrast to these results, radial modulations have been measured by a reciprocating double Langmuir probe on Tore Supra during the ergodic divertor operation (Fig. 1). Their main features are to be time independent, regular and with a large amplitude, roughly from 15 eV for minima up to 30 eV for maxima. In a standard 1D approach, one would be led to consider volume sources and sinks that would alternate regularly. Modulation locations seem to depend greatly on the shot conditions: a change in the magnetic equilibrium (major radius) led to an opposite phase between two successive shots (TS 15518 and TS 15519), which can be understood by the modification of the field lines connexion properties. The linear and decreasing profiles of the electronic density show that the particle transport does not drive or behave like the heat transport. Furthermore, the low values of the electronic density allow us to neglect radiative processes in order to explain the temperature modulations. Finally, one must remark that these modulations are not always measured.

On CSTNII, Langmuir probe measurements exhibit poloidal structure in the temperature field [1]. It is interesting to note that the poloidal period of these modulations (35°) corresponds to the main poloidal wave number (m = 10) of the magnetic perturbation. Similar observations have been made for Tore Supra, in a situation characterized by large overlapping of adjacent islands [2].

This poloidal pattern suggests that temperature modulations are governed by the structure of the field lines. This argument is backed by noting that the distance between two successive maxima roughly follows the distance between resonant locations computed with the quasi-linear theory (in the range of 0.02 m).

The third important feature concerns the effect of the divertor in the unperturbed region. According to the theoretical analysis, a drop of the temperature is expected in the core plasma, resulting from an increase of heat diffusivity which flattens out the temperature profile in the divertor volume. In contrast to this, Thomson scattering measurements on Text showed a temperature gradient increase at the separatrix and temperature that reach those of the limiter configuration values in the core [3]. A similar trend is observed on Tore Supra since the boundary temperature drop does not affect the core temperature profile.

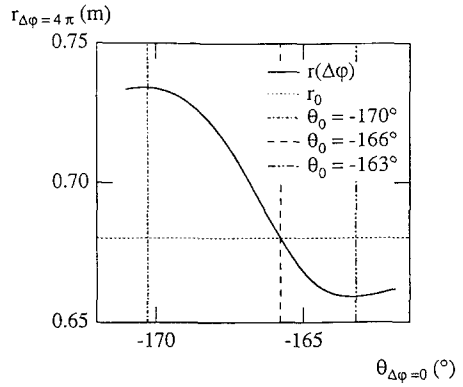

Fig. 2. Radial deflection of field lines for different initial poloidal locations and at r = 0.68 m.

3. Heat transport in a stochastic field as a superimposition of two diffusive networks

In order to link the temperature field and the structure of the field lines, the 3D MASTOC code has been used [4]. The code computes the magnetic perturbation induced by the ergodic divertor and adds it to the main magnetic field. One may then follow the field lines through their toroidal course and compute their final locations (Figs. 2 and 3). In order to take the transverse diffusion into account, the toroidal course is limited to a value corresponding to the Kolmogorov length.

On Fig. 2, the radial deflection is displayed for field lines initiated at a given radius but with different poloidal

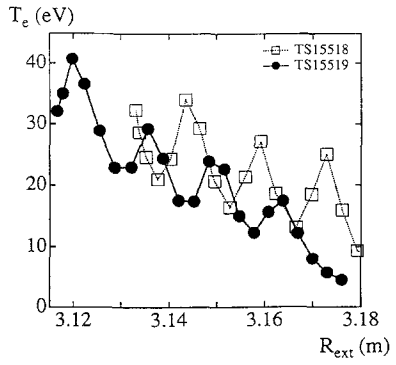

Fig. 1. Temperature profile on Tore Supra during ergodic divertor operation, measured with a reciprocating double Langmuir probe.

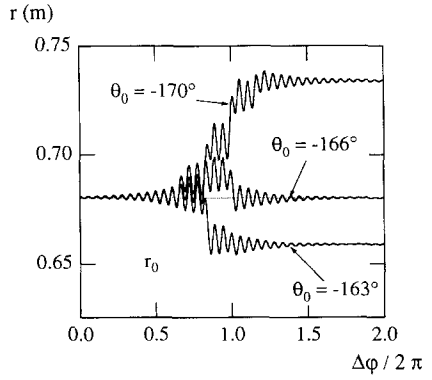

Fig. 3. Radial deflection for three field lines as a function of the toroidal angle (initial conditions are indicated on Fig. 2).

locations. Three particular trajectories are shown on Fig. 3: two are radially deflected either towards the wall or towards the plasma. The third one remains at the same radial location. Radial jumps induced by the stochasticity of the field lines are therefore only significant in specific poloidal regions. The same analysis can be made concerning the radial deflection of field lines that have initiated from the same poloidal location, but with different initial radial locations. This property of large radial jumps specifically localized in a poloidal section may be interpreted as a bidimensional network which stands for the parallel transport. One thus replaces a three dimensional problem by a two dimensional one. As a test particle can move on the deflected field lines towards the plasma core as well as towards the wall with an equal probability, the network can be considered as diffusive and will be called the *parallel connection network* (*PCN*). Though the connexion movement occurs in the radial direction, the term parallel is used to remind that radial jumps ($\Delta \sim$ of the order of 10^{-2} m) are governed by the parallel transport.

Let us consider a second network in the radial direction. This allows for a test particle either to reverse its parallel velocity so that the sites of the PCN can be connected in both directions, or to diffuse even if the particle is not affected by the PCN, which is clearly the case when the particles are located between two radial or poloidal successive sites of the PCN. This second network is called the *transverse diffusive network* (*TDN*) and is supposed to be spatially uniform with a characteristic step δ (typically a Larmor radius). In the following, we shall assume $\delta \ll \Delta$.

The superimposition of both networks may be restrained to a 1D model by introducing a probability p_θ which reflects the poloidal extent of the sites of the PCN. This probability would typically be given by the ratio $\delta y/y$ where δy is the poloidal characteristic width of a site and y, the distance between two successive sites in the poloidal direction. One may thus interpret p_θ as a measure of the capability for a test particle to enter the PCN.

In the case of superimposed networks, a test particle in the PCN is allowed to leave it and to enter in the TDN and reciprocally. To illustrate this situation, we consider the section of a flux tube and the effect of the magnetic perturbation on it. As a result of the stochasticity, the exponential divergence of neighbouring field lines leads to a spreading of the initial area. Very thin regions appear, while the measure of the whole area is conserved, as a consequence of $div\ B = 0$. When the characteristic scale of these regions is of the order of δ, the transverse diffusion tends to remove test particles from these areas. The coherence of the temperature field is bounded by such transverse diffusion process. We therefore introduce a second probability p_{stoch} measuring the capability for a test particle to remain in the PCN: $p_{\mathrm{stoch}} \sim \mathrm{d}S'/\mathrm{d}S$, where $\mathrm{d}S$ is the whole area and $\mathrm{d}S'$, the part of the area which has a typical scale significantly larger than δ.

The coupling between both networks can thus be expressed as a global probability: $p = p_\theta^* p_{\mathrm{stoch}}$.

In the following model, we study the diffusion of particles along the radial axis. Let r_{sep} be the location of the separatrix which bounds the stochastic region ($r > r_{\mathrm{sep}}$) and the unperturbed region ($r < r_{\mathrm{sep}}$). The latter is characterized by the existence of a standard diffusion (TDN) with a diffusion coefficient $D_\perp$, while the stochastic region contains the PCN in addition to the TDN. The origin $r = 0$ is the location of the energy influx Γ while on the other boundary at $r = L$, the wall is supposed to be perfectly absorbent.

From the previous section, it results that the probability p governs the profile of the test particles density, hence

$$p = \frac{\tilde{n}}{\tilde{n} + \bar{n}}, \tag{2}$$

where $\tilde{n}$ is the density of the test particles in the PCN and $\bar{n}$ the density in the TDN.

4. Test particles density profile

In the following, radial distances and densities are normalized by δ. In steady state, flux conservation may be written:

$$\Gamma = D_\perp \int_{r-\Delta}^{r} \tilde{n}(x)\,\mathrm{d}x - D_\perp \int_{r}^{r+\Delta} \tilde{n}(x)\,\mathrm{d}x - D_\perp \frac{\partial \bar{n}}{\partial r} \tag{3}$$

with the boundary condition $\bar{n}(L) = 0$.

Eq. (3) can be easily solved in the case of PCN sites with a vanishing width i.e., a PCN site extends over a single TDN site:

$$H(r) = \frac{p(r)}{1 - p(r)} = \sum_{k=0}^{w-1} H_k \delta(r - r_k),$$

where $\delta(r)$ represents the Dirac function and r_k the location of the k-site of the PCN. The last site is labelled by $w - 1$ and the first one by 0. The separatrix location is defined by $r_0 = r_{\mathrm{sep}}$.

One can find a relation between the density in the TDN in two successive sites:

$$(1 + H_{k+1}\Delta)\bar{n}_{k+1} = (1 + H_k \Delta)\bar{n}_k - \frac{\Gamma \Delta}{D_\perp} \quad \text{for } k < w - 1$$

Eq. (3) gives, for $r_{w-1} < r < L$:

$$\frac{\Gamma}{D_\perp} = H_{w-1}\bar{n}_{w-1} - \frac{\partial \bar{n}}{\partial r}$$

One then has, owing to the boundary condition:

$$\bar{n}(r = r_k) = \frac{1}{1 + H_k \Delta}\left(\frac{\Gamma}{D_\perp}(L - r_k) + \frac{\Gamma}{D_\perp}\zeta H_{w-1} \times \frac{\Delta - \zeta}{1 + \zeta H_{w-1}}\right) \tag{4}$$

where $\zeta = L - r_{w-1}$ expresses the distance between the last site and the wall.

The density in the PCN at each site can be deduced from the TDN, from Eq. (2). If the probability p is equal to zero everywhere (which is always the case in the unperturbed region), then $H_k = 0$ for any k and there is only one diffusion network. Eq. (4) then allows us to recover the result of a standard diffusion process (Eq. (1)), that is to say, a monotonous and decreasing profile.

5. Main results and discussion

In the following, profiles have been computed for a non-vanishing width of the PCN sites.

On Fig. 4, we show two profiles of the total density for different maximum probabilities (p_{max}) on the sites. For $p_{max} \sim 0.5$, one can recover steady state modulations. As p is further decreased, profiles tend to the limiter configuration (which is also the asymptotic case when $p = 0$). For $p_{max} \sim 0.05$, one can observe that these modulations have nearly disappeared. Since the probability accounts for the poloidal location, it may be concluded that radial modulations depend on the poloidal measurements. This may explain why some modulations are not always observed, as has been emphasized in Section 2.

Even though the maxima of the probability are localized on the sites, the maximum of the modulations are not. This is readily understood for sites with a non-vanishing width. Indeed, the front of the first site strongly weighs the local sink so that it is memorized all along the PCN. One then expects a phase-lag between the radial temperature modulations and the site locations in the PCN.

On Fig. 5, we represent for a given radius the test particles density as a function of the poloidal location, as determined by the poloidal dependence of the probability p_θ. For illustration, we choose $p = 1 - \alpha|\sin(n\theta)|$ with

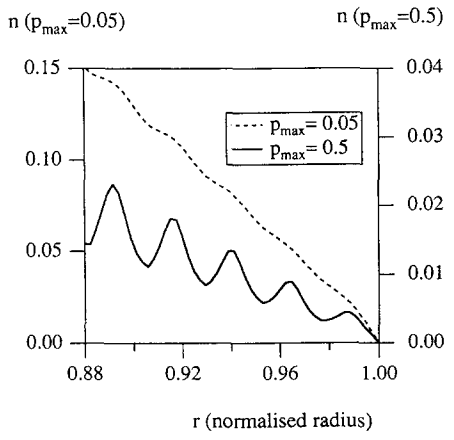

Fig. 4. Radial profile of test particle densities for two different values of the probability function.

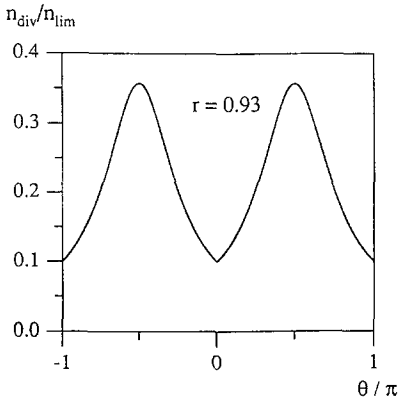

Fig. 5. Poloidal dependence of test particle densities for $p = 1 - 0.8|\sin\theta|$.

$n = 1$ and $\alpha = 0.8$. One can then remark that a low value of p leads to a strong test particles density decrease, so that the temperature field is also expected to be strongly dependent on the poloidal location and on the stochasticity level.

Since the divertor connexion properties exhibit a poloidal period locally governed by the resonant wave number, hence $m \sim 18$, it will induce the same periodicity for the probability. Thus, poloidal modulations are predicted by the model, as a consequence of the dependence of the test particles density on p. Of course, there is no reason for the probability to reach its extrema values 0 and 1. The p function is more likely bounded by $p_{min}(r)$ and $p_{max}(r)$, which determines the actual level of poloidal modulations.

Let us now consider the transition between the ergodic region ($r > r_0$) and the non-perturbed region ($r < r_0$). Eq. (4) allows us to compute the density at $r = r_0$, assuming that $H_0 = 0$. This simply results from the definition of the separatrix. The region before the separatrix satisfies the condition $p(r) = 0$ everywhere, in contrast to the region beyond the separatrix characterized by $p(r) \neq 0$.

One then has:

$$\bar{n}(r = r_0) = \frac{\Gamma}{D_\perp}(L - r_0) + \frac{\Gamma}{D_\perp}\zeta H_{w-1}\frac{\Delta - \zeta}{1 + \zeta H_{w-1}}$$

The first term in the right hand size of the equation is exactly the density at $r = r_0$ in a limiter configuration. Looking at the second term, one can easily remark that it is always greater or equal to zero. It can thus be concluded that $n(r_0) \geq n_{lim}(r_0)$. Equality occurs when ζ is equal to zero or Δ, which means that the final cell of the PCN is exactly located on the wall.

Because of the flattening of the test particles density in the ergodic region, this result leads to an increase of the gradient at the separatrix. The increase may be simply explained as resulting from a disymmetrical process be-

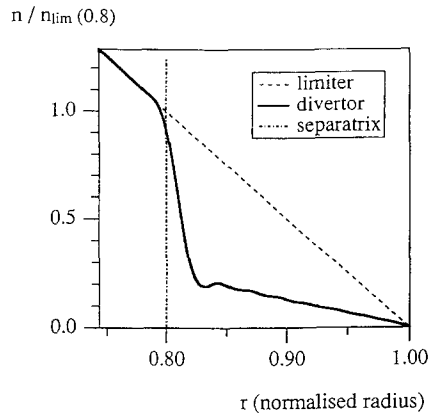

Fig. 6. Radial profiles of test particles in ergodic divertor and limiter configurations.

tween the first PCN site and the following one. Owing to the vanishing coherence of the first site, it does not send test particles outwards to the second site so that in this transition region, the diffusive process in the PCN is changed into an inward convection. We can thus conclude that the stochastic region generates a transport barrier which allows for a recovery of the confinement, in spite of the low confinement boundary associated to the stochastic region (Fig. 6). A similar result has been obtained experimentally from the analysis of impurity transport during the ergodic divertor operation on Tore Supra [5]. The observed improvement of the confinement is also attributed to an inward pinch in the vicinity of the separatrix.

The convective term Γ_{pinch} around the separatrix is computed with the following definition: $\Gamma_{\text{pinch}} = \Gamma + D_{\perp} \nabla \bar{n}$; the analytical calculation gives

$$\Gamma_{\text{pinch}} = -\Gamma \frac{H_1}{1 + H_1 \Delta} \left(L - r_1 + \zeta H_{w-1} \frac{\Delta - \zeta}{1 + \zeta H_{w-1}} \right)$$

As expected, the convective flux is negative, so that it generates a transport barrier and increases with the probability on the second site. The sharper the transition between the unperturbed/stochastic region, the more efficient is the barrier transport. We emphasize that the convection only exists in the vicinity of the separatrix in contrast to the two diffusive processes which govern the transport in the stochastic region.

6. Conclusion

The investigation of the field lines behaviour modified by a magnetic perturbation establishes that there are regions which are radially connected owing to the parallel transport. This connexion property is equivalent to a 2D network, composed by poloidally and radially localized sites. Taking a classical transverse diffusion into account, one can thus consider heat transport as a superimposition of two diffusion networks, with different characteristic scales. Neglecting all poloidal diffusion, it is possible to study the radial profile and its poloidal dependence by defining a probability which describes the poloidal locations of the test particles. A second probability coefficient is introduced in order to include the coupling between both networks, which stands for the balance between transverse diffusion and parallel transport. As such, it also governs the coherence loss along the parallel direction. A 1D model can then be defined in order to compute the density of test particles and to establish the main differences between the limiter and the ergodic divertor configuration. We show that the radial profile of the temperature field exhibits three regions.

The first one, the stochastic region between the wall and the separatrix, is characterized by modulations and by a lowered confinement as exemplified by the flat temperature profile. These modulations may be strongly attenuated depending on the poloidal location. The dependence of the test particles density on the probability generates poloidal modulations of the temperature, according to the poloidal modulations of the connexion properties.

A second region around the separatrix is characterized by an increase of the gradient resulting from a local convective phenomena (pinch effect) which allows for a compensation of the confinement loss in the stochastic region. In the third region, the core temperature field is unaffected.

References

[1] Takamura et al., J. Nucl. Mater. 162–164 (1989) 643.
[2] C. de Michelis et al., Control. Fusion 37 (1995) 505.
[3] T.E. Evans et al., J. Nucl. Mater. 145–147 (1987) 812.
[4] F. NGuyen, Ph. Ghendrih and A. Samain, Report EUR-CEA-FC-1539, Feb. (1995).
[5] M. Mattioli et al., Nucl. Fusion 35 (1995) 807.